

## Prognostic significance of genome-wide DNA methylation profiles within the randomized, phase 3, EORTC CATNON trial on non-1p/19q deleted anaplastic glioma

C. Mircea S. Tesileanu<sup>®</sup>, Martin J. van den Bent<sup>®</sup>, Marc Sanson, Wolfgang Wick<sup>®</sup>, Alba A. Brandes, Paul M. Clement, Sara C. Erridge, Michael A. Vogelbaum, Anna K. Nowak, Jean F. Baurain, Warren P. Mason, Helen Wheeler, Olivier L. Chinot, Sanjeev Gill, Matthew Griffin, Leland Rogers, Walter Taal, Roberta Rudà, Michael Weller<sup>®</sup>, Catherine McBain, Myra E. van Linde, Thais S. Sabedot, Yuri Hoogstrate, Andreas von Deimling, Iris de Heer, Wilfred F. J. van IJcken, Rutger W. W. Brouwer, Kenneth Aldape, Robert B. Jenkins<sup>®</sup>, Hendrikus J. Dubbink, Johan M. Kros, Pieter Wesseling, Kin Jip Cheung, Vassilis Gofinopoulos, Brigitta G. Baumert, Thierry Gorlia, Houtan Noushmehr,<sup>†®</sup> and Pim J. French<sup>†</sup>

Neurology Department, Erasmus MC, Rotterdam, the Netherlands (C.M.S.T., M.J.v.d.B., W.T., Y.H., I.d.H., P.J.F.); Sorbonne Université, Hôpitaux Universitaires La Pitié Salpêtrière, Paris, France (M.S.); Neurology Department, Universitätsklinikum Heidelberg, Heidelberg, Germany (W.W.); Medical Oncology Department, AUSL-IRCCS Scienze Neurologiche, Bologna, Italy (A.A.B.); Oncology Department, KU Leuven and Medical Oncology Department, UZ Leuven, Leuven, Belgium (P.M.C.); Neuro-Oncology Centre Edinburgh, Western General Hospital, Edinburgh, UK (S.C.E.); Neuro-Oncology Department, Moffitt Cancer Center, Tampa, Florida, USA (M.A.V.); University of Western Australia, Perth, Australia (A.K.N.); Co-Operative Group for Neuro-Oncology, University of Sydney, Sydney, Australia (A.K.N.); Medical Oncology Department, Sir Charles Gairdner Hospital, Nedlands, Australia (A.K.N.); Medical Oncology Department, King Albert II Cancer Institute, Cliniques universitaires Saint-Luc, Brussels, Belgium (J.F.B.); Princess Margaret Cancer Centre, Toronto, Ontario, Canada (W.P.M., K.A.); Northern Sydney Cancer Centre, Sydney, Australia (H.W.); Neuro-Oncology Department, Aix-Marseille University, Marseille, France (O.L.C.); Medical Oncology Department, Alfred Hospital, Melbourne, Australia (S.G.); Clinical Oncology Department, Nottingham University Hospitals NHS Trust, Nottingham, UK (M.G.); Radiation Oncology Department, Gammawest Cancer Services, Salt Lake City, Utah, USA (L.R.); Neuro-Oncology Department, University of Turin, Turin, Italy (R.R.); Neurology Department, University Hospital of Zurich, Zurich, Switzerland (M.W.); Clinical Oncology Department, The Christie NHS Foundation Trust, Manchester, UK (C.M.); Medical Oncology Department, Amsterdam UMC, Amsterdam, the Netherlands (M.E.v.L.); Neurosurgery Department, Henry Ford Health System, Detroit, Michigan, USA (T.S.S., H.N.); Neuropathology Department, Ruprecht-Karls-University, Heidelberg, Germany (A.v.D.); Clinical Cooperation Unit Neuropathology, German Cancer Consortium (DKTK), German Cancer Research Center (DKFZ), Heidelberg, Germany (A.v.D.); Biomics Center, Erasmus MC, Rotterdam, the Netherlands (W.F.J.v.I.J., R.W.W.B.); Pathology Department, Mayo Clinic, Rochester, Minnesota, USA (R.B.J.); Pathology Department, Erasmus MC, Rotterdam, the Netherlands (H.J.D., J.M.K.); Pathology Department, Amsterdam UMC, Amsterdam, the Netherlands (P.W.); Princess Máxima Center, Utrecht, the Netherlands (P.W.); EORTC HQ, Brussels, Belgium (K.J.C., V.G., T.G.); Radiation Oncology Department, Maastricht UMC, Maastricht, the Netherlands (B.G.B.); Radiation Oncology Institute, Cantonal Hospital Graubünden, Chur, Switzerland (B.G.B.)

<sup>†</sup>These authors contributed equally to this work.

**Corresponding Author:** Pim J. French, PhD, Neurology Department, Brain Tumor Center, Erasmus MC Cancer Institute, 's-Gravendijkwal 230, 3015 CE Rotterdam, the Netherlands ([p.french@erasmusmc.nl](mailto:p.french@erasmusmc.nl)).

### Abstract

**Background.** Survival in patients with *IDH1/2*-mutant (*mt*) anaplastic astrocytomas is highly variable. We have used the prospective phase 3 CATNON trial to identify molecular factors related to outcome in *IDH1/2mt* anaplastic astrocytoma patients.

**Methods.** The CATNON trial randomized 751 adult patients with newly diagnosed 1p/19q non-codeleted anaplastic glioma to 59.4 Gy radiotherapy +/- concurrent and/or adjuvant temozolomide. The presence of necrosis and/or

microvascular proliferation was scored at central pathology review. Infinium MethylationEPIC BeadChip arrays were used for genome-wide DNA methylation analysis and the determination of copy number variations (CNV). Two DNA methylation-based tumor classifiers were used for risk stratification. Next-generation sequencing (NGS) was performed using 1 of the 2 glioma-tailored NGS panels. The primary endpoint was overall survival measured from the date of randomization.

**Results.** Full analysis (genome-wide DNA methylation and NGS) was successfully performed on 654 tumors. Of these, 432 tumors were *IDH1/2mt* anaplastic astrocytomas. Both epigenetic classifiers identified poor prognosis patients that partially overlapped. A predictive prognostic Cox proportional hazard model identified that independent prognostic factors for *IDH1/2mt* anaplastic astrocytoma patients included; age, mini-mental state examination score, treatment with concurrent and/or adjuvant temozolomide, the epigenetic classifiers, *PDGFRA* amplification, *CDKN2A/B* homozygous deletion, *PI3K* mutations, and total CNV load. Independent recursive partitioning analysis highlights the importance of these factors for patient prognostication.

**Conclusion.** Both clinical and molecular factors identify *IDH1/2mt* anaplastic astrocytoma patients with worse outcome. These results will further refine the current WHO criteria for glioma classification.

### Key Points

1. DNA methylation profiles have prognostic relevance for *IDH1/2mt* anaplastic astrocytoma patients.
2. Integration of clinical data, DNA methylation profiles, and genetic data is needed for accurate prognostication of *IDH1/2mt* anaplastic astrocytoma patients.

### Importance of the Study

Grading of diffuse *IDH1/2mt* glioma is still done by classical morphology, apart from homozygous deletion (HD) of *CDKN2A/B* that is correlated with a poor outcome and which is proposed by the cIMPACT-NOW committee as a criterion for *IDH1/2mt* astrocytoma, grade 4. Identifying other molecular factors associated with outcome within tumor entities potentially allows for more precise prognostication of histologically similar tumors. We used the randomized CATNON trial to test the prognostic significance of several alterations within

a homogeneously treated group of patients diagnosed with *IDH1/2mt* anaplastic astrocytoma. Tumor-related factors associated with an inferior outcome were identified by 2 different DNA methylation classifiers, as well as HD of *CDKN2A/B*, *PDGFRA* amplification, *PI3K* mutations, and total CNV load. In contrast to histological indicators of high grade, these molecular markers were significant in multivariable analysis and therefore can be used to identify patients with poor prognosis.

The diagnosis of gliomas has shifted from histology alone toward the incorporation of molecular data in the revised World Health Organization (WHO) 2016 classification of brain tumors, initially with isocitrate dehydrogenase 1 and 2 (*IDH1/2*) mutational status and the presence or absence of combined loss of the 1p and 19q chromosomal arms (1p/19q codeletion). This classification was found to be more objective, reproducible, and correlated better with outcome compared to classical histology.<sup>1-3</sup> Still, even within the well-defined molecular subsets of glioma, significant and clinically relevant differences in outcome exist. Homozygous deletion (HD) of cyclin-dependent kinase inhibitor 2 A and B (*CDKN2A/B*) has recently been identified in *IDH1/2*-mutant (*mt*) astrocytoma as a first molecular marker of grade 4 clinical behavior.<sup>4-6</sup> Numerous other genetic markers have been proposed to further prognosticate *IDH1/2mt* astrocytoma

patients, in particular retinoblastoma 1 (*RB1*) pathway alterations, tyrosine-protein kinase Met (*MET*) amplification (*amp*), N-myc proto-oncogene (*MYCN*) amplification, platelet-derived growth factor receptor alpha (*PDGFRA*) amplification, phosphatidylinositol 3-kinase (*PI3K*) mutations, and total copy number variation (CNV) load.<sup>4-10</sup> At the epigenetic level, tumor-specific genome-wide cytosine-phosphate-guanine (CpG) methylation patterns have been identified in diffuse glioma. Two classification systems have been reported that make use of the epigenetic profile to diagnose brain tumor subtypes: (1) a DNA methylation-based classification of all central nervous system (CNS) tumors by Capper et al. (named here: “the CNS tumor classifier”), and (2) a DNA methylation-based classification of gliomas by Ceccarelli et al. which can be supplemented with a risk to progression stratification from glioma-CpG island methylator

phenotype (G-CIMP)-high to G-CIMP-low as reported by de Souza et al. (combined, named here: “the glioma classifier”).<sup>11–14</sup> The accuracy of these molecular characteristics in relation to outcome has thus far not been clinically validated in homogeneously treated cohorts of patients. We therefore aimed to test and evaluate the importance of reported prognostic genetic and epigenetic molecular markers within the CATNON trial, the largest prospective study conducted on anaplastic astrocytoma patients.<sup>15</sup> These validated subtypes can be used for prognostication and results can be considered for the grading of tumors of the CNS.

## Methods

### Study Design and Participants

The CATNON trial is a 2 × 2 factorial design, non-blinded, multicenter (n = 137), randomized clinical trial in adult patients (n = 751) with primary 1p/19q non-codeleted anaplastic gliomas conducted by the European Organisation for Research and Treatment of Cancer (EORTC).<sup>15</sup> After local diagnosis of an anaplastic glioma, tumor samples were submitted prior to randomization for central pathology review of the tumor grade, and for central testing of O<sup>6</sup>-methylguanine DNA methyltransferase (*MGMT*) promoter methylation status. The absence of combined 1p/19q loss was either determined by local testing or at central review. Patients were computer-generated randomized (1:1:1:1) to radiotherapy alone (59.4 Gy in 33 fractions of 1.8 Gy), radiotherapy with concurrent temozolomide (75 mg/m<sup>2</sup> daily, max 7 weeks), radiotherapy with adjuvant temozolomide (12 4-week cycles: 150–200 mg/m<sup>2</sup> on days 1–5), or radiotherapy with both concurrent and adjuvant temozolomide.

### Compliance With Ethical Standards

All institutions obtained ethics approval from their institutional review boards or ethics review committees before enrollment started. All patients gave written informed consent according to local, national, and international guidelines.

### Procedures

DNA was isolated from formalin-fixed paraffin-embedded (FFPE) tumor samples as described previously.<sup>16</sup> *IDH1/2*, B-Raf proto-oncogene serine/threonine-protein kinase (*BRAF*), H3.3 histone A (*H3F3A*), *CDKN2A/B*, *RB1*, *PI3K* subunit alpha (*PIK3CA*), and *PI3K* regulatory subunit 1 (*PIK3R1*) mutation status were determined from either 1 of the 2 glioma-tailored next-generation sequencing (NGS) panels as described previously.<sup>17,18</sup> DNA methylation profiling was performed with the Infinium MethylationEPIC BeadChip according to the manufacturer’s instructions after using the Infinium FFPE DNA Restoration Kit. CNV data (*CDKN2A/B* HD, *RB1* HD, cyclin-dependent kinase 4 (*CDK4*) amp, cyclin-dependent kinase 6 (*CDK6*) amp, *MET* amp,

*MYCN* amp, *PDGFRA* amp) were derived from the DNA methylation data. *MGMT* promoter status was assessed with the *MGMT*-STP27 algorithm.<sup>19</sup> Samples that did not pass quality control, ie, the signal detection *P* value was <.01 in more than 5% of the probes were excluded from further analysis. HDs and amplifications were defined as ±0.60 log<sub>2</sub> intensity differences. CNV differences between ±0.60 and ±0.30 log<sub>2</sub> intensity were visually inspected for CNV calling, blinded to all other molecular or clinical data. DNA methylation-based epigenetic subtyping was established using random forest modeling using a classifier described by Capper et al., and one classifier described by Ceccarelli et al.<sup>11,12</sup> The latter classifier was supplemented with the risk of progression from G-CIMP-high to G-CIMP-low based on beta values of 7 specific CpGs as described previously (named here: “risk tumors” and “no-risk tumors”).<sup>13</sup> Total CNV load was calculated as described previously with a threshold for loss and gain of ±0.10 log<sub>2</sub> intensity on the CNV plot and a cutoff of 350 Mb.<sup>20</sup> Two dedicated neuropathologists scored the presence or absence of necrosis and microvascular proliferation at the central pathology review (J.M.K.: European and Australian samples, K.A.: North American samples). Clinical data such as survival, sex, age at enrollment, use of corticosteroids at enrollment (no use vs stable/decreasing dose), type of surgery (biopsy vs resection), mini-mental state examination (MMSE) score at enrollment (<27 vs 27–30), and treatment regimen were collected from the study entry forms.

### Statistical Analysis

The primary endpoint for all correlations of the epigenetic subtypes, DNA mutations and CNV was overall survival (OS), measured from the date of randomization until the date of death or censored at the date of last follow-up. Survival curves were created using the Kaplan-Meier technique and compared with the log-rank test. The Cox regression model was used for univariable and multivariable analysis to determine hazard ratios (HR) with 95% confidence intervals (CI), and significance was assessed with the likelihood ratio test. Factors with likelihood ratio test *P* values ≤.10 and at least 2 subgroups with n > 5 were taken into consideration for multivariable analysis. Principal component analysis (PCA) was performed on the 20 000 most variable probes between samples. The *t*-distributed stochastic neighbor embedding (*t*-SNE) plot was created with all significant probes at detection *P* value <.01 except those with lower overall reliability as previously described by Zhou et al.<sup>21</sup> The prognostic prediction models were made using stepwise backward elimination. Schoenfeld’s test was utilized to assess proportional hazard (PH) assumptions of Cox PH models. Harrell’s concordance index (C-index) was calculated and bootstrapped by 1000 iterations for the final models. Recursive partitioning analysis was performed on the significant factors from univariable analysis with 10 cross-validations in which every leaf had n > 20 patients. For all non-specified analyses, *P* values below .05 were considered significant. Statistical analysis was performed using R version 3.6.3 and packages *minfi*, *stats*, *rms*, *survival*, *Rtsne*, and *rpart*. This trial is registered with ClinicalTrials.gov, number NCT00626990. Upon



completion of all ongoing analyses, all data will be made available upon request at EORTC headquarters.

## Results

### Cohort Description

Comparison of the patient cohorts with and without molecular data identified that those able to be analyzed were younger (median age: 41 years vs 47 years,  $P = .006$ ) and more likely to have had debulking surgery (82.6% vs 58.8%,  $P < .0001$ ), but all other factors were similar (Supplementary Table 1). Genome-wide DNA methylation analysis was successfully performed on 654 samples of the 751 patients (19 samples were of low quality, and for 78 patients, there was insufficient tumor tissue available, Supplementary Figures 1 and 2). Of these, 440 (67.3%) were *IDH1/2mt*, 204 (31.2%) were *IDH1/2* wild type (*wt*), and for 10, the *IDH1/2* status could not be determined (Figure 1A, B and Supplementary Figure 1). Copy number assessment identified 8 (1.2%) *IDH1/2mt* anaplastic oligodendroglioma leaving 432 *IDH1/2mt* anaplastic astrocytomas. Ten *IDH1/2wt* tumors had an *H3F3A K27M* mutation and 4 had an *H3F3A G34R* mutation. Three *IDH1/2wt* tumors had a *BRAF* mutation (2 *V600E* and 1 *R509Q*) and 1 *IDH1/2mt* tumor had a *BRAF* mutation (*K601E*). Central histology review identified necrosis and/or microvascular proliferation, consistent with grade 4 tumors, in 95 (14.5%) samples (38 *IDH1/2wt*, 57 *IDH1/2mt*; in 40 necrosis, and in 79 microvascular proliferation; Figure 2F and Supplementary Figure 3A). PCA of the DNA methylation data primarily showed division between *IDH1/2wt* and *IDH1/2mt* gliomas in the first primary component accounting for 51% of variance in all samples (Figure 1B). Clinical characteristics of the cohort are listed in Table 1.

At the time of database lock (May 7, 2019), 31 *IDH1/2wt* anaplastic astrocytoma patients (15.2%), 288 *IDH1/2mt* anaplastic astrocytoma patients (66.7%), and 8 *IDH1/2mt* anaplastic oligodendroglioma patients (100%) were still alive. Median OS was 1.7 years (95% CI 1.4-1.9) for *IDH1/2wt* anaplastic astrocytoma patients and 8.2 years (95% CI 7.1-not reached) for *IDH1/2mt* anaplastic astrocytoma patients (HR 6.95, 95% CI 5.51-8.78;  $P < .0001$ ).

### DNA Methylation Analysis of All Samples

The majority of samples were assigned by “the CNS tumor classifier” to lower-grade (WHO 2 or 3) *IDH1/2mt* astrocytomas (A\_IDH,  $n = 317$ ) or high-grade (WHO 3 or 4) *IDH1/2mt* astrocytomas (A\_IDH\_HG,  $n = 113$ ). Other diagnoses according to “the CNS tumor classifier” were methylation class family *IDH1/2wt* glioblastomas (MTCF\_GBM,  $n = 161$ ), *H3F3Amt G34R* gliomas (GBM\_G34,  $n = 5$ ), *H3F3Amt K27M* gliomas (DMG\_K27,  $n = 11$ ), 1p/19q codeleted gliomas (O\_IDH,  $n = 12$ ), and 35 tumors with other, more rare diagnoses. Of note, not all classifications were considered equally reliable: in 74 samples the main class calibrated score was below 0.836, which has been described as the lower bound for an optimal sensitivity and specificity.<sup>12</sup> When only samples meeting this calibration

score were taken into account, the classifications correlated even better with molecular features. For example, all 4 DMG\_K27 tumors with a reliability score below 0.836 did not show an *H3F3A K27M* mutation in the NGS analysis, whereas the mutation was confirmed in all 7 tumors with a calibrated score  $\geq 0.836$  (Figure 1D).

The different epigenetic subtypes are highly correlated with patient survival: median OS in patients with A\_IDH not reached (95% CI 8.0-not reached), with A\_IDH\_HG 5.6 years (95% CI 4.0-not reached), with DMG\_K27 3.3 years (95% CI 2.3-not reached), with GBM\_G34 1.4 years (95% CI 1.0-not reached), with MTCF\_GBM 1.4 years (95% CI 1.3-1.8), with O\_IDH 9.1 years (too few events to estimate the CI), and with the combination of other diagnoses 2.4 years (95% CI 1.8-5.5; Figure 2A, B). The difference in OS between patients with the molecularly highly similar tumors A\_IDH and A\_IDH\_HG tumors was highly significant (A\_IDH\_HG vs A\_IDH: HR 2.43, 95% CI 1.73-3.40;  $P < .0001$ ).

We next assigned the 654 tumors into subgroups based on “the glioma classifier,” to 409 G-CIMP-high tumors, 19 G-CIMP-low tumors, 18 codel tumors, 107 mesenchymal-like tumors, 48 classic-like tumors, and 53 pilocytic astrocytoma (PA)-like/glioblastoma-like glioma methylation group 6 (“LGm6-GBM”) tumors. The latter subdiagnosis is combined as it requires additional histology review to determine the presence or absence of necrosis and/or microvascular proliferation for further separation. After this central histology review, the subgroup is further separated into 41 PA-like tumors and 12 LGm6-GBM tumors. The PA-like tumors were not a single nosological entity; in this set, we identified 9 tumors with *H3F3A* mutations (7 *K27M*, 2 *G34R*) and 1 *BRAF*-mutated tumor (*R509Q*). The LGm6-GBM tumors also contained 2 tumors with *H3F3A* mutations (*K27M*) and 1 tumor with a *BRAF* mutation (*V600E*).

“The glioma classifier” tumor subtypes were also strongly associated with patient survival: OS in patients with G-CIMP-high 9.5 years (95% CI 7.5-not reached), with G-CIMP-low 2.8 years (95% CI 2.0-not reached), with codel 9.1 years (too few events to estimate the CI), with mesenchymal-like 1.3 years (95% CI 1.2-1.7), with classic-like 1.6 years (95% CI 1.4-1.8), and with PA-like/LGm6-GBM 2.8 years (95% CI 2.1-3.7; Figure 2C, D). Particularly notable was the difference in OS between G-CIMP status subgroup patients (G-CIMP-low vs G-CIMP-high: HR 4.12, 95% CI 2.37-7.18;  $P < .0001$ ). PA-like/LGm6-GBM tumor patients had better outcome than mesenchymal-like and classic-like tumor patients (HR 0.42, 95% CI 0.28-0.62;  $P < .0001$ , and HR 0.38, 95% CI 0.24-0.59;  $P < .0001$ , respectively), suggesting a positive prognostic epigenetic subgroup within *IDH1/2wt* astrocytomas. This survival benefit remained for both the PA-like and the LGm6-GBM tumors after separation by central histology review of this group (Supplementary Figure 3B). Using the G-CIMP-low risk to progression profile, we classified 116 of the 409 G-CIMP-high tumors (28.4%) as “risk tumors” (Supplementary Figure 4). Patients harboring “risk tumors” had a worse outcome compared to “no-risk tumor” patients: median OS of 6.9 years (95% CI 5.7-not reached) in risk tumor patients vs not reached (95% CI 8.0-not reached) in no-risk tumor patients (risk vs no-risk: HR 1.64, 95% CI 1.13-2.37;  $P = .01$ ; Figure 2E).

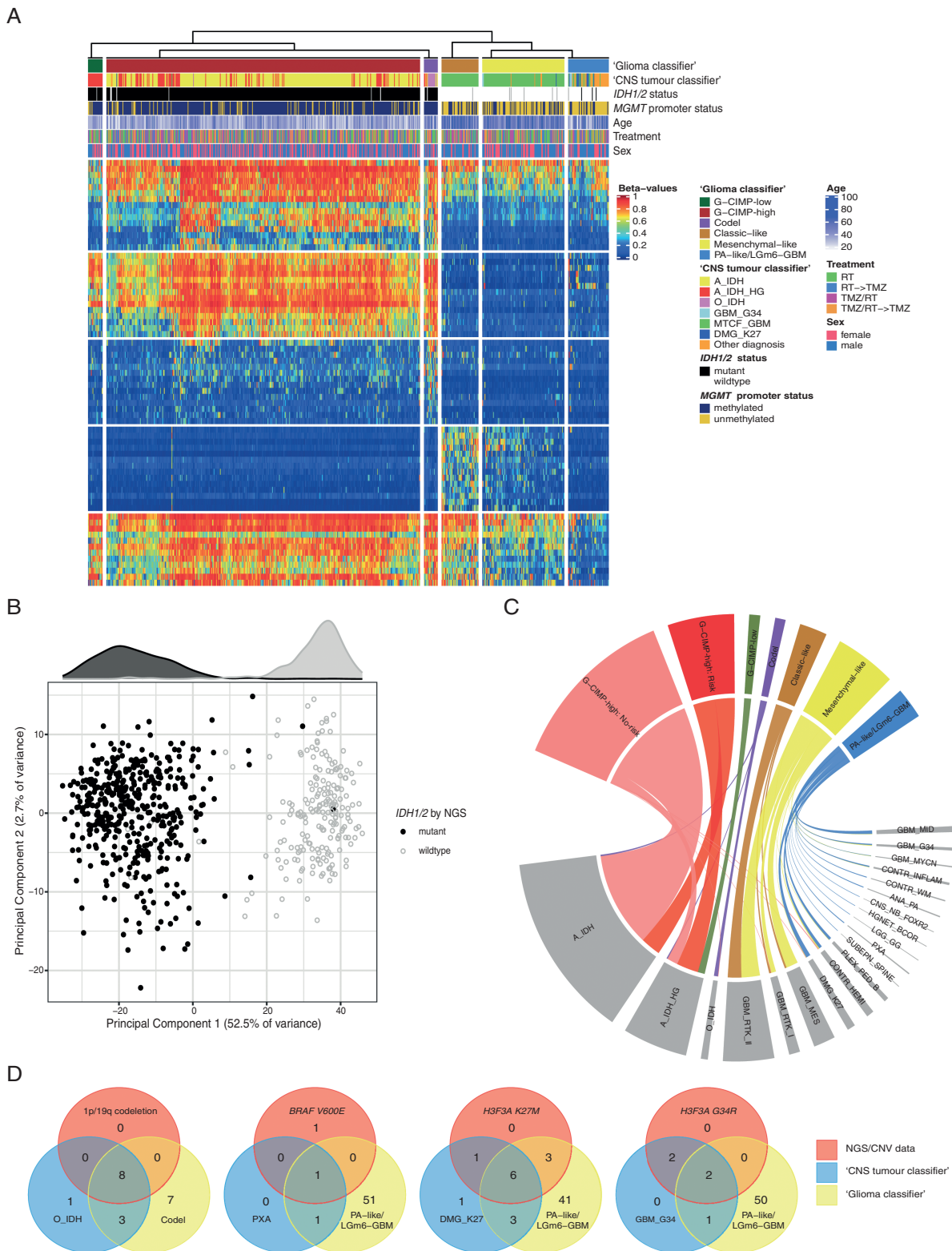


**Fig. 1** Epigenetic subtyping of all CATNON samples that had molecular data available and passed quality control. (A) DNA methylation heatmap of discriminative probes for “glioma classifier” subtypes shows a clear overlap between the different classifiers, and a strong correlation with *IDH1/2* status, *MGMT* promoter status, and patient age. (B) Principal component analysis of the 20 000 most variable probes illustrates separation of the epigenetic data on *IDH1/2* status. (C) Circle plot shows a high degree of correlation between “glioma classifier” and “CNS tumor classifier”

Although both classifiers were generated independently, there is a large overlap between the epigenetic subtypes of “the CNS tumor classifier” and “the glioma classifier” (Figure 1A, C, D). For example, every G-CIMP-low tumor was classified as an A\_IDH\_HG tumor, and 11/12 (91.7%) O\_IDH tumors were classified as codel tumors. All classic-like tumors and 100/107 (93.5%) mesenchymal-like tumors were MTCF\_GBM tumors, whereas 404/409 (98.8%) G-CIMP-high tumors were A\_IDH or A\_IDH\_HG tumors. “Risk tumors” (n = 61) were mainly A\_IDH\_HG tumors and most “no-risk tumors” (n = 258) were A\_IDH tumors (odds ratio 9.47, 95% CI 5.46-16.73;  $P < .0001$ ). The major difference between the 2 classifiers are those tumors that “the CNS tumor classifier” does not identify as MTCF\_GBM, A\_IDH, A\_IDH\_HG or O\_IDH (n = 51), or tumors with a main diagnosis reliability score  $< 0.836$  (n = 74): most of these tumors (n = 41 and n = 31, respectively) were labeled PA-like/LGm6-GBM tumors.

To explore potential prognostic differences between “the CNS tumor classifier” and “the glioma classifier,” we stratified “the CNS tumor classifier” classes by “the glioma classifier” subtypes and vice versa (Supplementary Figure 5). Within the A\_IDH\_HG tumors, those assigned to G-CIMP-low had a significantly worse OS compared to those assigned to G-CIMP-high regardless of progression risk. There were, however, no differences in OS when either A\_IDH or A\_IDH\_HG tumors were stratified by risk to G-CIMP-low progression (log-rank test between G-CIMP-high: No-risk and G-CIMP-high: Risk of Supplementary Figure 5A, B:  $P = .33$  and  $P = .42$ , respectively). Stratifying “risk tumors” and “no-risk tumors” into “the CNS tumor classifier” subgroups showed a significant OS difference in both A\_IDH and A\_IDH\_HG tumors (HR 1.80 95% CI 1.01-3.21,  $P = .06$ ; and HR 2.00 95% CI 1.06-3.77,  $P = .03$ , respectively).

### Analysis of the *IDH1/2mt* Anaplastic Astrocytoma Cohort

We set out to build a prognostic model specifically for *IDH1/2mt* anaplastic astrocytoma patients. Although a *t*-SNE plot of only the 432 *IDH1/2mt* anaplastic astrocytomas does not separate these epigenetic subtypes, they do have a distinct spatial distribution within this plot (Figure 3A and Supplementary Figure 6). We further performed NGS

and CNV analysis and identified 43 *IDH1/2mt* anaplastic astrocytomas with *CDKN2A/B* HD, 6 with *RB1* HD, 25 with *CDK4amp*, 22 with *PDGFRAamp*, 7 with *METamp*, 7 with *MYCNamp*, 4 with *CDK6amp*, and 20 with *PI3K* mutations (14 *PIK3R1*, 6 *PIK3CA*). The total CNV load was classified as high in 185 (42.8%) *IDH1/2mt* anaplastic astrocytomas based on an algorithm by Shirahata et al.<sup>20</sup>

Univariable analysis of the *IDH1/2mt* anaplastic astrocytomas showed that most of the clinical, molecular, and histological factors were associated with OS, ie, age groups, WHO performance score, MMSE, type of surgery, use of corticosteroids, treatment with adjuvant temozolomide, treatment with concurrent temozolomide, the presence of necrosis and/or microvascular proliferation, “the CNS tumor classifier,” “the glioma classifier,” *CDK4amp*, *METamp*, *PDGFRAamp*, *CDKN2A/B* HD, *PI3K* mutations, and total CNV load (Supplementary Table 2, Figure 2F, Supplementary Figures 7 and 8). Only patient sex, *MGMT* promoter methylation, *MYCNamp*, and *RB1* HD were not associated with OS at univariable analysis (with the latter 2 factors present in only a few cases). The presence of the prognostic molecular and histological markers correlated with DNA methylation classes A\_IDH\_HG tumors, G-CIMP-low tumors, and G-CIMP-low progression risk (Figure 3B). Moreover, several of the prognostic molecular and histological markers showed significant co-occurrence.

Cox PH models made by stepwise backward elimination of significant factors from univariable analysis resulted in 3 multivariable models with independent significant factors: (1) the clinical/histological model (using the clinical and histological factors), (2) the tissue-based model (using the molecular and histological factors), and (3) the combined model (using clinical, molecular, and histological factors). The final clinical/histological model included age groups, WHO performance score, treatment with adjuvant temozolomide, the presence of necrosis and/or microvascular proliferation, and type of primary surgery and had a bootstrap corrected C-index of 0.626, while the final tissue-based model included “the CNS tumor classifier,” “the glioma classifier,” *PDGFRAamp*, *CDKN2A/B* HD, *PI3Kmt*, and total CNV load with a bootstrap corrected C-index of 0.665. However, the predictive final combined model performed markedly better than both the clinical/histological and the tissue-based model

diagnoses. (D) Venn diagrams showing the correlation between “the glioma classifier,” “the CNS tumor classifier,” and genetic changes. CNS, central nervous system; *IDH1/2*, isocitrate dehydrogenase 1 and 2; *MGMT*, O<sup>6</sup>-methylguanine DNA methyltransferase; G-CIMP, glioma-CpG island methylator phenotype; No-risk, no-risk of progression to G-CIMP-low; Risk, risk of progression to G-CIMP-low; Codel, 1p/19q codeleted; PA-like/LGm6-GBM, pilocytic astrocytoma-like/glioblastoma-like glioma methylation group 6; A\_IDH, *IDH1/2mt*-like astrocytomas lower-grade; A\_IDH\_HG, *IDH1/2mt*-like astrocytomas high-grade; O\_IDH, *IDH1/2mt*-like oligodendrogliomas; *IDH1/2mt*, *IDH1/2* mutant; GBM\_G34, *H3F3Amt G34R*-like tumor; MTCF\_GBM, methylation class family *IDH1/2wt* glioblastomas; DMG\_K27, *H3F3Amt K27M*-like tumor; *H3F3Amt*, H3.3 histone A mutant; RT, radiotherapy; RT->TMZ, radiotherapy with adjuvant temozolomide; RT/TMZ, radiotherapy with concurrent temozolomide; TMZ/RT->TMZ, radiotherapy with concurrent and adjuvant temozolomide; NGS, next-generation sequencing; GBM\_RTK\_1, glioblastoma, receptor tyrosine kinase 1 alterations; GBM\_RTK\_2, glioblastoma, receptor tyrosine kinase 2 alterations; GBM\_MES, glioblastoma, mesenchymal; CONTR\_HEMI, control tissue, hemispheric cortex; PLEX\_PED\_B, plexus tumor, pediatric subtype B; SUBEPN\_SPINE, subependymoma, spine; PXA, pleomorphic xanthoastrocytoma; LGG\_GG, low-grade glioma, ganglioglioma; HGNET\_BCOR, high-grade neuroepithelial tumor with *BCOR* alteration; *BCOR*, *BCL6* corepressor; CNS\_NB\_FOXR2, CNS neuroblastoma with *FOXR2* activation; *FOXR2*, forkhead box R2; ANA\_PA, anaplastic pilocytic astrocytoma; CONTR\_WM, control tissue, white matter; CONTR\_INFLAM, control tissue, inflammatory tumor microenvironment; GBM\_MYCN, glioblastoma, *MYCN* alterations; *MYCN*, N-myc proto-oncogene; GBM\_MID, glioblastoma, midline; *BRAF*, B-Raf proto-oncogene serine/threonine-protein kinase; CNV, copy number variation.

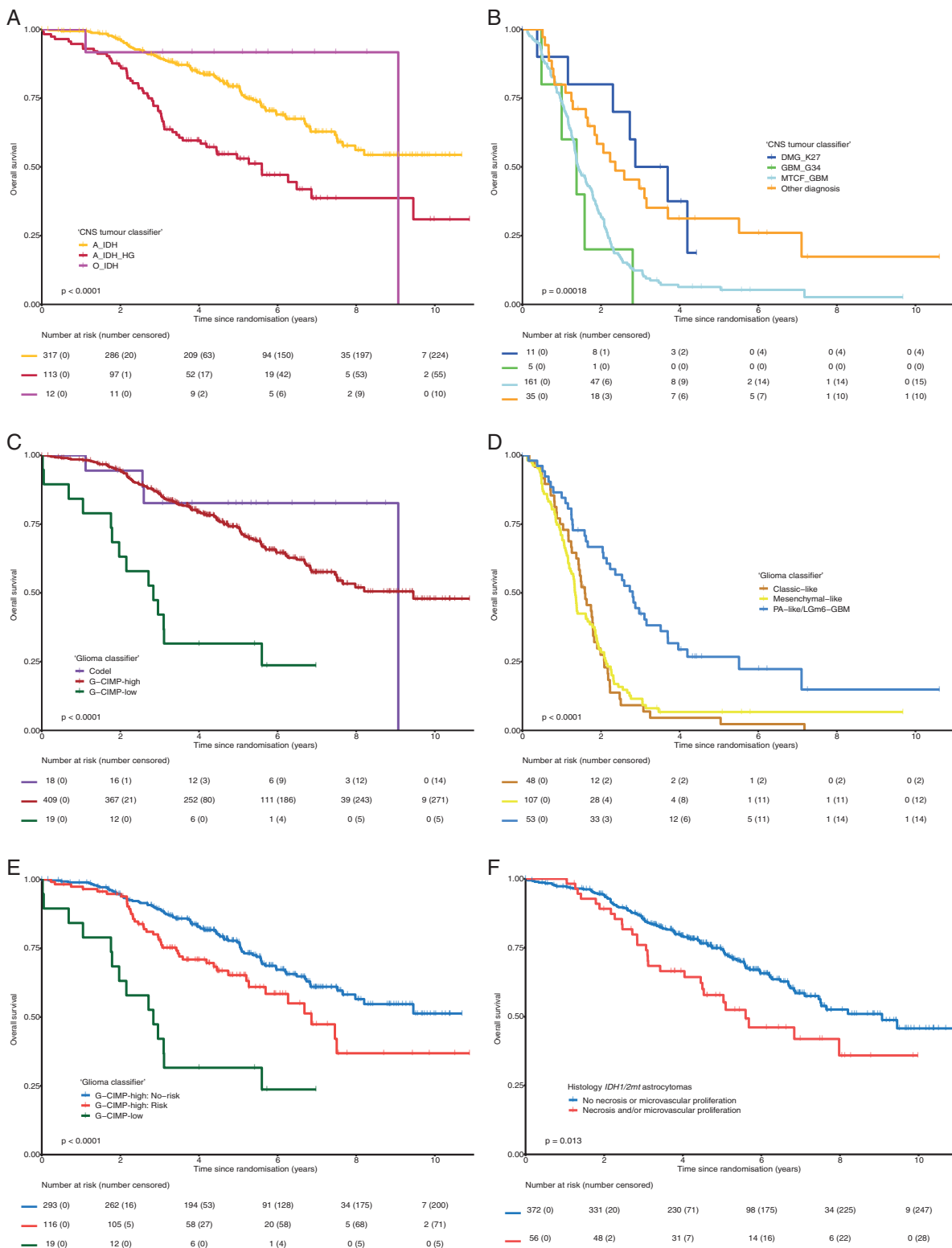


**Fig. 2** Kaplan-Meier curves of CATNON stratified by DNA methylation class demonstrate prognostic relevance of epigenetic profiling. (A) Overall survival of A\_IDH, A\_IDH\_HG, and O\_IDH tumor patients. (B) Overall survival of DMG\_K27, GBM\_G34, MTCF\_GBM, and other diagnosis tumor patients. (C) Overall survival of Codel, G-CIMP-high, and G-CIMP-low tumor patients. (D) Overall survival of classic-like, mesenchymal-like, and PA-like/LGm6-GBM tumor patients. (E) Overall survival of G-CIMP-high: No-risk, G-CIMP-high: Risk, and G-CIMP-low tumor patients. (F)



**Table 1** Baseline Clinical Characteristics Included Patients Divided by Treatment Regimen

	Radiotherapy Alone	Radiotherapy With Concurrent Temozolomide	Radiotherapy With Adjuvant Temozolomide	Radiotherapy With Adjuvant and Concurrent Temozolomide	P Value	All Patients
Patients, n	168	162	159	165		654
Sex, n (%)					0.657 <sup>a</sup>	
Female	69 (41.1)	61 (37.7)	68 (42.8)	73 (44.2)		271 (41.4)
Male	99 (58.9)	101 (62.3)	91 (57.2)	92 (55.8)		383 (58.6)
Age, y					0.196 <sup>b</sup>	
Median (range)	42 (19-81)	43 (20-77)	39 (20-82)	40 (18-72)		41 (18-82)
IDH1/2 status, n (%)					0.795 <sup>a</sup>	
Mutant	107 (63.7)	110 (67.9)	108 (67.9)	115 (69.7)		440 (67.3)
Wild type	57 (33.9)	49 (30.2)	49 (30.8)	49 (29.7)		204 (31.2)
Missing	4 (2.4)	3 (1.9)	2 (1.3)	1 (0.6)		10 (1.5)
MGMT promoter, n (%)					0.94 <sup>a</sup>	
Methylated	116 (69)	107 (66)	109 (68.6)	113 (68.5)		445 (68)
Unmethylated	52 (31)	55 (34)	50 (31.4)	52 (31.5)		209 (32)
WHO performance score, n (%)					0.851 <sup>a</sup>	
0	96 (57.1)	94 (58)	92 (57.9)	102 (61.8)		384 (58.7)
>0	71 (42.3)	68 (42)	66 (41.5)	63 (38.2)		268 (41)
Missing	1 (0.6)	0 (0)	1 (0.6)	0 (0)		2 (0.3)
Type of surgery, n (%)					0.448 <sup>a</sup>	
Biopsy	26 (15.5)	35 (21.6)	27 (17)	26 (15.8)		114 (17.4)
Resection	142 (84.5)	127 (78.4)	132 (83)	139 (84.2)		540 (82.6)
Use of corticosteroids, n (%)					0.814 <sup>a</sup>	
Yes	44 (26.2)	48 (29.6)	40 (25.2)	46 (27.9)		178 (27.2)
No	124 (73.8)	114 (70.4)	118 (74.2)	119 (72.1)		475 (72.6)
Missing	0 (0)	0 (0)	1 (0.6)	0 (0)		1 (0.2)
Necrosis and/or microvascular proliferation, n (%)					0.178 <sup>a</sup>	
Present	30 (17.9)	26 (16)	23 (14.5)	16 (9.7)		95 (14.5)
Absent	136 (81)	133 (82.1)	135 (84.9)	145 (87.9)		549 (83.9)
Missing	2 (1.2)	3 (1.9)	1 (0.6)	4 (2.4)		10 (1.5)

**Abbreviations:** IDH1/2, isocitrate dehydrogenase 1 and 2; MGMT, O<sup>6</sup>-methylguanine DNA methyltransferase; WHO, World Health Organization.

<sup>a</sup>Fisher exact test. <sup>b</sup>Wilcoxon rank sum test.

with a bootstrapped C-index of 0.709, and included age group, MMSE, treatment with concurrent temozolomide, treatment with adjuvant temozolomide, "the CNS tumor classifier," "the glioma classifier," *PDGFRAamp*, *CDKN2A/B* HD, *PI3Kmt*, and total CNV load. The final clinical/histological and combined models are illustrated as Forest plots in [Figure 4](#). Schoenfeld's tests for individual variables and the

total model of the combined model were nonsignificant ([Supplementary Figure 9](#)). The final tissue-based model is illustrated in [Supplementary Figure 10](#).

Finally, we performed recursive partitioning analysis on the significant factors from univariable analysis to create a prognostic decision tree for *IDH1/2mt* anaplastic astrocytoma patients. The first split of the tree is made

Overall survival of *IDH1/2mt* anaplastic astrocytoma patients: necrosis and/or microvascular proliferation vs no necrosis or microvascular proliferation. CNS, central nervous system; A\_IDH, *IDH1/2mt*-like astrocytomas lower-grade; A\_IDH\_HG, *IDH1/2mt*-like astrocytomas high-grade; O\_IDH, *IDH1/2mt*-like oligodendrogliomas; *IDH1/2mt*, isocitrate dehydrogenase 1 and 2 mutant; DMG\_K27, *H3F3Amt K27M*-like tumor; GBM\_G34, *H3F3Amt G34R*-like tumor; *H3F3Amt*, H3.3 histone A mutant; MTCF\_GBM, glioblastoma; Codel, 1p/19q codeleted; G-CIMP, glioma-CpG island methylator phenotype; PA-like/LGm6-GBM, pilocytic astrocytoma-like/glioblastoma-like glioma methylation group 6; No-risk, no-risk of progression to G-CIMP-low; Risk, risk of progression to G-CIMP-low.



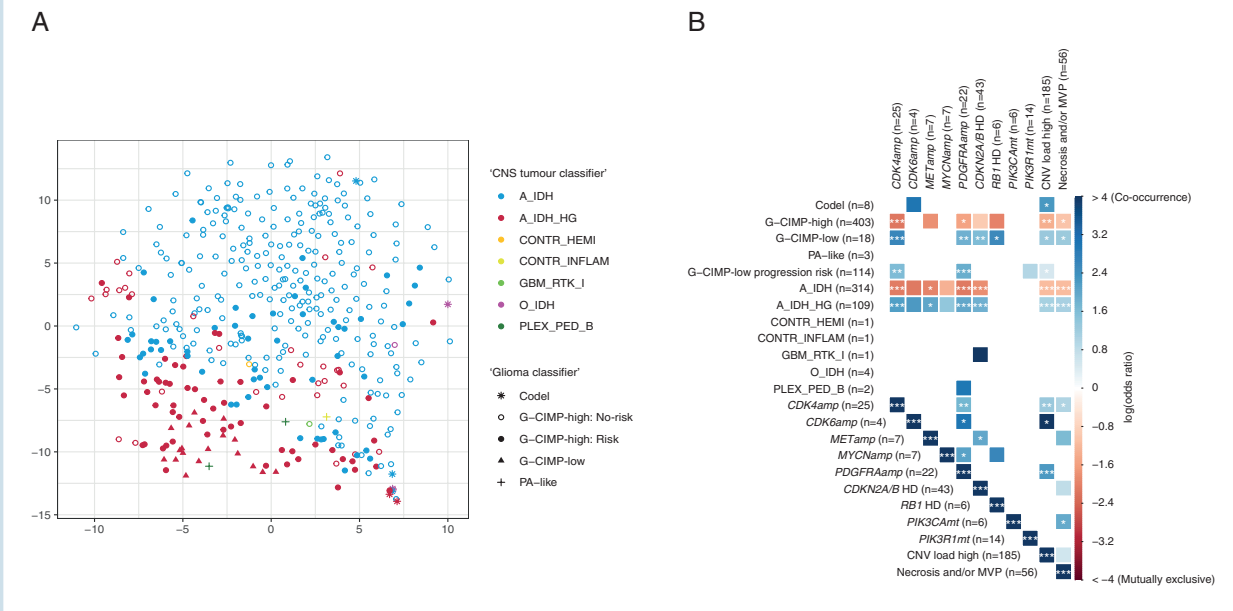


**Fig. 3** Detailed molecular analysis of *IDH1/2mt* anaplastic astrocytomas of CATNON. (A) *t*-distributed stochastic neighbor embedding plot of all *IDH1/2mt* anaplastic astrocytomas. Samples are colored by “CNS tumor classifier” subgroup with shapes representing “glioma classifier” subgroups. Although no subgroups are clearly distinguishable in this plot, specific classifier subgroups show spatial segregation. (B) Correlation plot of DNA methylation data, genetic data, and histology. A\_IDH\_HG and G-CIMP-low tumors correlate with both molecular and histological markers of malignancy. Nonsignificant correlations (ie, Fisher exact test  $\geq 0.10$ ) were removed from this plot. CNS, central nervous system; A\_IDH, *IDH1/2mt*-like astrocytomas lower-grade; A\_IDH\_HG, *IDH1/2mt*-like astrocytomas high-grade; *IDH1/2mt*, isocitrate dehydrogenase 1 and 2 mutant; CONTR\_HEMI, control tissue, hemispheric cortex; CONTR\_INFLAM, control tissue, inflammatory tumor microenvironment; GBM\_RTJ, glioblastoma, receptor tyrosine kinase 1 alterations; O\_IDH, *IDH1/2mt*-like oligodendrogliomas; PLEX\_PED\_B, plexus tumor, pediatric subtype B; Codel, 1p/19q codeleted; G-CIMP, glioma-CpG island methylator phenotype; No-risk, no-risk of progression to G-CIMP-low; Risk, risk of progression to G-CIMP-low; PA-like, pilocytic astrocytoma-like; amp, amplification; *CDK4*, cyclin-dependent kinase 4; *CDK6*, cyclin-dependent kinase 6; *MET*, tyrosine-protein kinase Met; *MYCN*, N-myc proto-oncogene; *PDGFRA*, platelet-derived growth factor receptor alpha; HD, homozygous deletion; *CDKN2A/B*, cyclin-dependent kinase inhibitor 2 A and B; *RB1* HD, retinoblastoma 1; *mt*, mutant; *PIK3CA*, phosphatidylinositol 3-kinase subunit alpha; *PIK3R1*, phosphatidylinositol 3-kinase regulatory subunit 1; CNV, copy number variation; MVP, microvascular proliferation. \* = 0.10 > *P*  $\geq 0.05$ , \*\* = 0.05 > *P*  $\geq 0.01$ , \*\*\* = *P* < 0.01.

on the presence/absence of *CDKN2A/B* HD highlighting the importance of this molecular marker for prognostication. Additional branches are made by treatment with adjuvant temozolomide, WHO performance score, and “the CNS tumor classifier,” resulting in 3 clinically relevant subgroups with either a fair outcome, intermediate outcome, or poor outcome (Figure 5). Recursive partitioning analysis of solely the *IDH1/2mt* anaplastic astrocytoma cohort that was treated with adjuvant temozolomide did not result in a stable model and is therefore not shown here.

## Discussion

Our study used tissue samples from the prospective randomized CATNON trial to validate the prognostic relevance of DNA methylation-based epigenetic subtyping by both “the CNS tumor classifier” and “the glioma classifier” in a cohort of homogeneously treated anaplastic glioma patients. We demonstrate that, in *IDH1/2mt* anaplastic astrocytoma patients, both DNA methylation classifiers, alone or in combination with clinical data as well as other

molecular markers (*PI3K* mutation status, and CNV analysis of *PDGFRA*, *CDKN2A/B*, and CNV load) exhibit prognostic significance. Our study validates the OS difference of A\_IDH and A\_IDH\_HG tumor patients, the negative prognostic impact of the G-CIMP-low methylation profile, and the negative prognostic impact of the risk to G-CIMP-low progression score.

This validation is important, as both “the CNS tumor classifier” and “the glioma classifier” are available and can be easily used to diagnose and prognosticate new tumor samples with locally assessed DNA methylation data.<sup>12,22</sup> The clear prognostic importance of the DNA methylation-based subgroups in *IDH1/2mt* anaplastic astrocytoma suggests consideration for implementation in standard glioma diagnostics. Importantly, the added predictive effect of *PDGFRA*amp, *CDKN2A/B* HD, total CNV load, and *PI3K* mutation status can be considered as an integral part of prognosticating (“grading”) *IDH1/2mt* anaplastic astrocytomas. For example, both the G-CIMP-low methylation profile and HD of *CDKN2A/B* were shown to be negative prognostic markers, yet only in patients harboring tumors with the combination of these markers does the OS resemble the outcome in grade

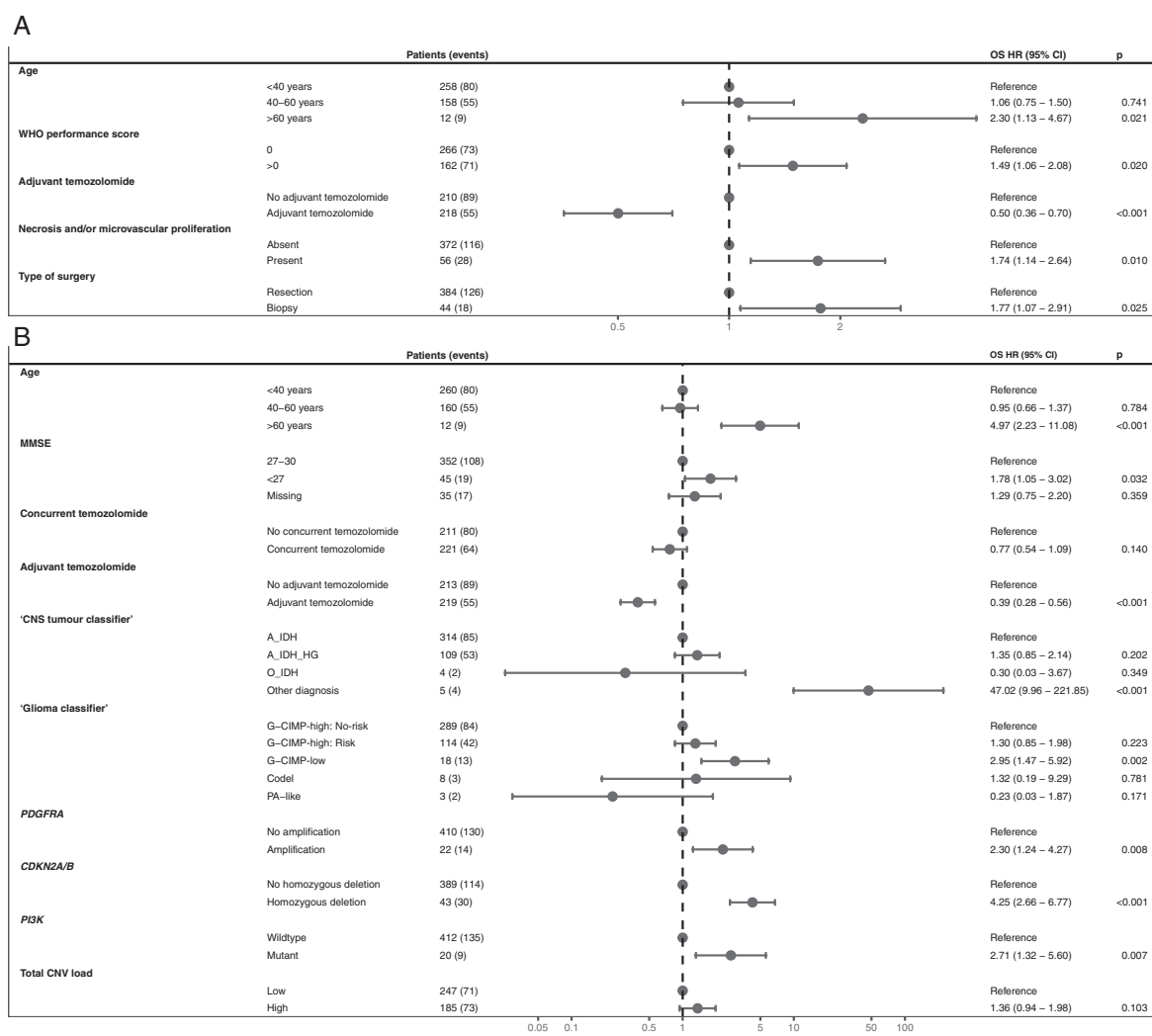


**Fig. 4** Forest plots of predictive Cox proportional hazard models for *IDH1/2mt* anaplastic astrocytoma patients. (A) The clinical/histological model based on clinical and histological variables. Four out of 432 *IDH1/2mt* anaplastic astrocytoma patients were missing histological data and were subsequently omitted from this final model due to incorporation of necrosis and/or microvascular proliferation as a significant factor. (B) The combined model based on clinical, molecular, and histological variables. *IDH1/2mt*, isocitrate dehydrogenase 1 and 2 mutant; OS, overall survival; HR, hazard ratio; CI, confidence interval; WHO, World Health Organization; MMSE, mini-mental state examination score; CNS, central nervous system; A\_IDH, *IDH1/2mt*-like astrocytomas lower-grade; A\_IDH\_HG, *IDH1/2mt*-like astrocytomas high-grade; O\_IDH, *IDH1/2mt*-like oligodendrogliomas; G-CIMP, glioma-CpG island methylator phenotype; No-risk, no-risk of progression to G-CIMP-low; Risk, risk of progression to G-CIMP-low; Codel, 1p/19q codeleted; PA-like, pilocytic astrocytoma-like; *PDGFRA*, platelet-derived growth factor receptor alpha; *CDKN2A/B*, cyclin-dependent kinase inhibitor 2 A and B; *PI3K*, phosphatidylinositol 3-kinase; CNV, copy number variation.

4 *IDH1/2wt* glioma patients as described in previous research.<sup>23</sup>

Within *IDH1/2wt* anaplastic astrocytoma, the prognostic PA-like/LGm6-GBM subgroup of “the glioma classifier” was assessed as well. Both *BRAF* mutations and *H3F3A* mutations were identified in these tumors showing heterogeneity in this subgroup, since these mutations are indicative of both better and worse outcome patients.<sup>3,24,25</sup> This heterogeneity is further emphasized by the overlap with sporadic diagnoses from “the CNS tumor classifier” with low reliability scores. These findings show that some tumors of this group cannot be classified by epigenetics and

they require classification based on NGS and/or CNV data. Further analysis of *IDH1/2wt* anaplastic gliomas of the CATNON trial and outcome to treatment will be reported separately elsewhere.

The limitations of this study are predominantly the limited number of survival events within the *IDH1/2mt* anaplastic astrocytoma patients, a lack of longitudinal tissue analysis, the absence of external validation of our predictive prognostic model, and the limited number of several investigated molecular markers. Although the OS of the epigenetic subtypes in the present dataset so far confirms previous observations, a longer-term follow-up of

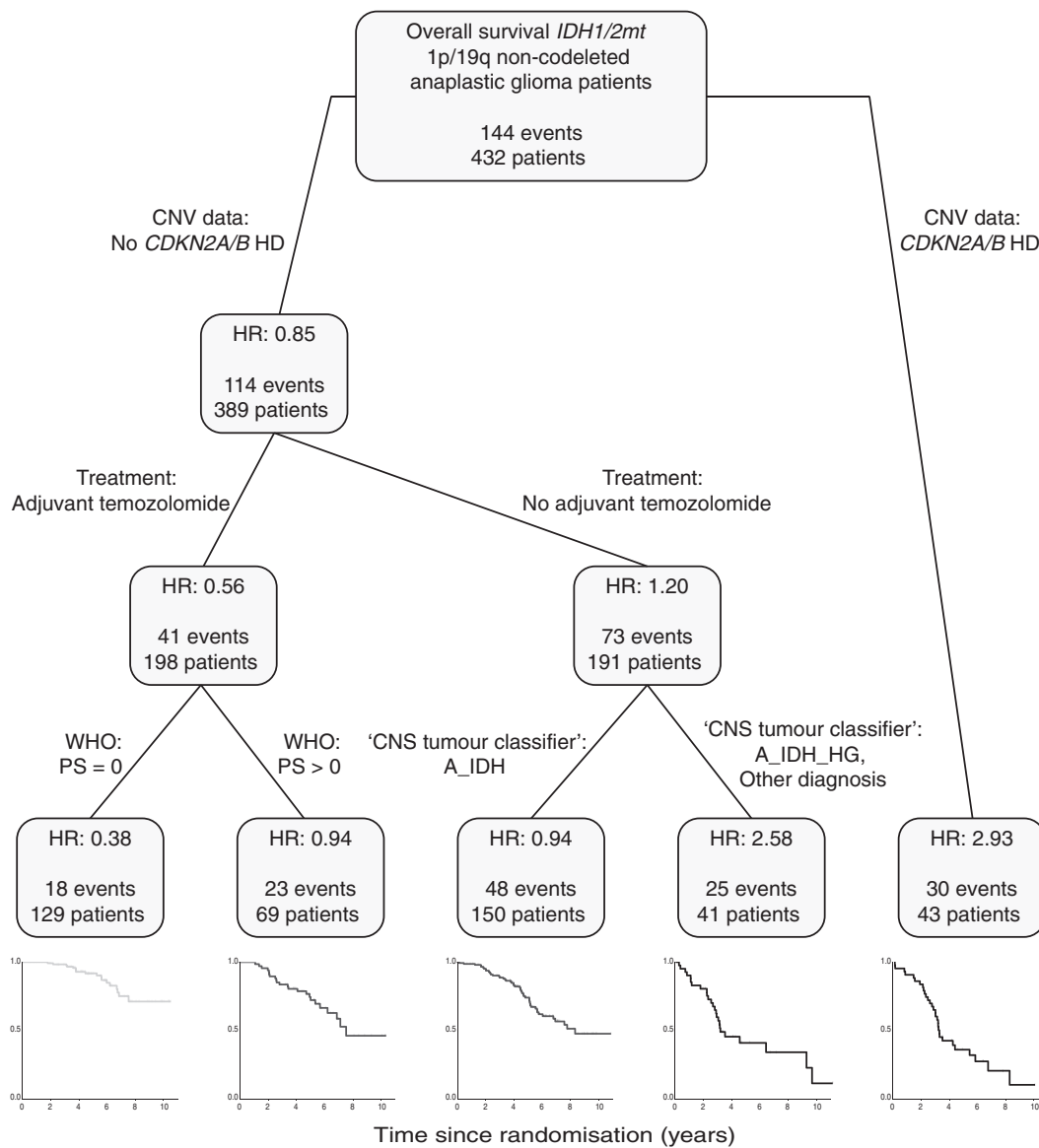


**Fig. 5** Recursive partitioning analysis of the clinical, histological and molecular factors for *IDH1/2mt* anaplastic astrocytoma patients with HRs respective to entire cohort. Prognostic subgroups have been color-coded for outcome: light gray is fair, dark gray is intermediate, and black is poor. *IDH1/2mt*, isocitrate dehydrogenase 1 and 2 mutant; CNV, copy number variation; *CDKN2A/B*, cyclin-dependent kinase inhibitor 2 A and B; HD, homozygous deletion; HR, hazard ratio; WHO, World Health Organization; PS, performance score; CNS, central nervous system; A\_IDH, *IDH1/2mt*-like astrocytomas lower-grade; A\_IDH\_HG, *IDH1/2mt*-like astrocytomas high-grade.

this study will aim to validate our findings.<sup>11,13</sup> Longitudinal analysis is required to determine how many tumors at risk to progression to G-CIMP-low indeed have progressed to this subtype. Though there is no external validation of our combined predictive model, the model has been generated in the largest cohort of *IDH1/2mt* anaplastic astrocytoma patients to date and all evaluated prognostic markers were previously identified in *IDH1/2mt* astrocytomas. Another limitation is the focus of the CATNON trial on grade 3 tumors, as one might argue that the conclusions of this study cannot be extrapolated to grade 2 and 4 *IDH1/2mt* astrocytomas. However, the histological criteria used

for grading are prone to interobserver and intraobserver variability, and most samples were reviewed by 2 central pathologists who at times disagreed about the grade. Additionally, some centers were allowed to enter patients on a local diagnosis from which the central reviewers deviated. As a consequence, the study enrolled cases that either bordered on grade 2 or on grade 4 tumors, and even cases with some necrosis and/or microvascular proliferation were enrolled. Although necrosis and microvascular proliferation are criteria for grade 4 tumors, the dedicated central neuropathologists diagnosed some tumors as grade 3 in the presence of these histological abnormalities.

This apparent discrepancy reflects the difficulty in tumor grading and therefore this dataset represents a broader range of tumors than strict grade 3.

In short, DNA methylation-based epigenetic subtyping by “the glioma classifier” and “the CNS tumor classifier” in combination with clinical and genetic data has added value in prognosticating and diagnosing *IDH1/2mt* anaplastic astrocytomas. These epigenetic subtypes and molecular markers should therefore be considered for incorporation within the next WHO classification of CNS tumors.

## Supplementary Material

Supplementary material is available at *Neuro-Oncology* online.

## Keywords

1p/19q non-codeleted | anaplastic glioma | DNA methylation profiling | *IDH* mutant | patient prognostication

## Funding

This study was supported by MSD (educational grant, provision of temozolomide), the NRG (grants U10CA180868 and U10CA180822), Cancer Research UK (grant CRUK/07/028), and Cancer Australia (grants 1026842 and 1078655). The molecular analysis was funded by The Brain Tumour Charity (grant GN-000577), the Dutch Cancer Society (grant 10685), the Vereniging Heino “Strijd van Salland,” and the USA Department of Defence (grant CA170278).

## Acknowledgments

We thank our patients and their relatives for their willingness to participate in this study; all sites and their staff; the EORTC Headquarters staff, the NRG Oncology staff; the Australian NHMRC Clinical Trials Centre staff; the HBTC staff; and the MRC Clinical Trials Unit staff.

**Conflict of interest statement.** M.J.v.d.B.: grants Dutch Cancer Foundation, Brain Tumor Charity, Strijd van Salland, MSD; personal fees Carthera, Nerviano, Bayer, Celgene, Agios, AbbVie, Karyopharm, Boston Pharmaceuticals, Genenta. P.M.C.: personal fees Bristol-Meyers Squibb, AbbVie, Merck Serono, MSD, Vifor Pharma, Daiichi Sankyo, LEO Pharma, AstraZeneca, Takeda. M.A.V.: royalty rights and indirect equity Infuseon Therapeutics, personal fees Tocagen, Celgene. A.K.N.: grants AstraZeneca, Douglas Pharmaceuticals, travel funding AstraZeneca, Boehringer Ingelheim, consulting fees Douglas Pharmaceuticals, Bayer Pharmaceuticals, Pharmabincine, Atara Biotherapeutics, Trizell Ltd., payment to institution Douglas Pharmaceuticals, Atara Biotherapeutics,

steering committee fees Roche Pharmaceuticals, Boehringer Ingelheim. O.L.C.: personal fees AbbVie, nonfinancial support AbbVie, Immatics, BMS. R.R.: advisory board fees UCB, Novocure. M.W.: grants AbbVie, Adastr, Dracen, MSD, Merck, Novocure, personal fees AbbVie, MSD, Merck, Basilea, Bristol-Meyers Squibb, Celgene, Medac, Nerviano Medical Sciences, Orbus, Philogen, Roche, Tocagen. A.v.D.: antibody patent *IDH1<sup>R132H</sup>*, *BRAF<sup>V600E</sup>*. H.J.D.: personal fees AbbVie. B.G.B.: personal fees Roche, nonfinancial support Roche. Other authors: no competing interests.

**Authorship statement.** Study design: C.M.S.T., M.J.v.d.B., A.v.D., B.G.B., T.G., H.N., and P.J.F. Data collection: C.M.S.T., M.J.v.d.B., M.S., W.W., A.A.B., P.M.C., S.C.E., M.A.V., A.K.N., J.F.B., W.P.M., H.W., O.L.C., S.G., M.G., L.R., W.T., R.R., M.W., C.M., M.E.v.L., I.d.H., W.F.J.v.I.J., R.W.W.B., K.A., R.B.J., H.J.D., J.M.K., P.W., K.J.C., V.G., B.G.B., H.N., and P.J.F. Data analysis: C.M.S.T., M.J.v.d.B., I.d.H., T.S.S., Y.H., H.N., and P.J.F. Data interpretation: C.M.S.T., M.J.v.d.B., T.S.S., T.G., and P.J.F. Writing/approving final manuscript: all authors.

## References

- Smith JS, Perry A, Borell TJ, et al. Alterations of chromosome arms 1p and 19q as predictors of survival in oligodendrogliomas, astrocytomas, and mixed oligoastrocytomas. *J Clin Oncol*. 2000;18(3):636–645.
- Yan H, Parsons DW, Jin G, et al. *IDH1* and *IDH2* mutations in gliomas. *N Engl J Med*. 2009;360(8):765–773.
- Louis DN, Perry A, Reifenberger G, et al. The 2016 World Health Organization classification of tumors of the central nervous system: a summary. *Acta Neuropathol*. 2016;131(6):803–820.
- Reis GF, Pekmezci M, Hansen HM, et al. *CDKN2A* loss is associated with shortened overall survival in lower-grade (World Health Organization Grades II-III) astrocytomas. *J Neuropathol Exp Neurol*. 2015;74(5):442–452.
- Appay R, Dehais C, Maurage CA, et al. *CDKN2A* homozygous deletion is a strong adverse prognosis factor in diffuse malignant *IDH*-mutant gliomas. *Neuro Oncol*. 2019;21(12):1519–1528.
- Brat DJ, Aldape K, Colman H, et al. *cIMPACT-NOW* update 5: recommended grading criteria and terminologies for *IDH*-mutant astrocytomas. *Acta Neuropathol*. 2020;139(3):603–608.
- Phillips JJ, Aranda D, Ellison DW, et al. *PDGFRA* amplification is common in pediatric and adult high-grade astrocytomas and identifies a poor prognostic group in *IDH1* mutant glioblastoma. *Brain Pathol*. 2013;23(5):565–573.
- Draaisma K, Wijnenga MM, Weenink B, et al. *PI3* kinase mutations and mutational load as poor prognostic markers in diffuse glioma patients. *Acta Neuropathol Commun*. 2015;3:88.
- Aoki K, Nakamura H, Suzuki H, et al. Prognostic relevance of genetic alterations in diffuse lower-grade gliomas. *Neuro Oncol*. 2018;20(1):66–77.
- Yang RR, Shi ZF, Zhang ZY, et al. *IDH* mutant lower grade (WHO Grades II/III) astrocytomas can be stratified for risk by *CDKN2A*, *CDK4* and *PDGFRA* copy number alterations. *Brain Pathol*. 2020;30(3):541–553.
- Ceccarelli M, Barthel FP, Malta TM, et al. Molecular profiling reveals biologically discrete subsets and pathways of progression in diffuse glioma. *Cell*. 2016;164(3):550–563.



12. Capper D, Jones DTW, Sill M, et al. DNA methylation-based classification of central nervous system tumours. *Nature*. 2018;555(7697):469–474.
13. de Souza CF, Sabedot TS, Malta TM, et al. A distinct DNA methylation shift in a subset of glioma CpG island methylator phenotypes during tumor recurrence. *Cell Rep*. 2018;23(2):637–651.
14. Noushmehr H, Weisenberger DJ, Diefes K, et al. Identification of a CpG island methylator phenotype that defines a distinct subgroup of glioma. *Cancer Cell*. 2010;17(5):510–522.
15. van den Bent MJ, Baumert B, Erridge SC, et al. Interim results from the CATNON trial (EORTC study 26053-22054) of treatment with concurrent and adjuvant temozolomide for 1p/19q non-co-deleted anaplastic glioma: a phase 3, randomised, open-label intergroup study. *Lancet*. 2017;390(10103):1645–1653.
16. Draaisma K, Chatzipli A, Taphoorn M, et al. Molecular evolution of IDH wild-type glioblastomas treated with standard of care affects survival and design of precision medicine trials: a report from the EORTC 1542 Study. *J Clin Oncol*. 2020;38(1):81–99.
17. Dubbink HJ, Atmodimedjo PN, van Marion R, et al. Diagnostic detection of allelic losses and imbalances by next-generation sequencing: 1p/19q co-deletion analysis of gliomas. *J Mol Diagn*. 2016;18(5):775–786.
18. Sahn F, Schrimpf D, Jones DT, et al. Next-generation sequencing in routine brain tumor diagnostics enables an integrated diagnosis and identifies actionable targets. *Acta Neuropathol*. 2016;131(6):903–910.
19. Bady P, Delorenzi M, Hegi ME. Sensitivity analysis of the MGMT-STP27 model and impact of genetic and epigenetic context to predict the MGMT methylation status in gliomas and other tumors. *J Mol Diagn*. 2016;18(3):350–361.
20. Shirahata M, Ono T, Stichel D, et al. Novel, improved grading system(s) for IDH-mutant astrocytic gliomas. *Acta Neuropathol*. 2018;136(1):153–166.
21. Zhou W, Laird PW, Shen H. Comprehensive characterization, annotation and innovative use of Infinium DNA methylation BeadChip probes. *Nucleic Acids Res*. 2017;45(4):e22.
22. Colaprico A, Silva TC, Olsen C, et al. TCGAbiolinks: an R/Bioconductor package for integrative analysis of TCGA data. *Nucleic Acids Res*. 2016;44(8):e71.
23. Li KK, Shi ZF, Malta TM, et al. Identification of subsets of IDH-mutant glioblastomas with distinct epigenetic and copy number alterations and stratified clinical risks. *Neurooncol Adv*. 2019;1(1):vdz015.
24. Khuong-Quang DA, Buczkowicz P, Rakopoulos P, et al. K27M mutation in histone H3.3 defines clinically and biologically distinct subgroups of pediatric diffuse intrinsic pontine gliomas. *Acta Neuropathol*. 2012;124(3):439–447.
25. Broniscer A, Baker SJ, West AN, et al. Clinical and molecular characteristics of malignant transformation of low-grade glioma in children. *J Clin Oncol*. 2007;25(6):682–689.